Energy Equip. Sys./ Vol. 12/No. 3/September 2024/ 197-216

ENERGY EQUIPSYS

Energy Equipment and Systems

www.energyequipsys.com

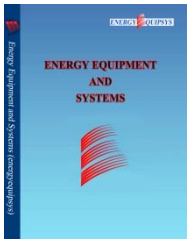

Thermodynamic investigation on coal fired emission free s-CO_2 power cycles

Manuscript Type

Research Paper

Authors

Anand Pavithran[a]
Meeta Sharma[a*]
Anoop Kumar Shukla[a]

Amity University Uttar Pradesh, Noida, India

Article history:

Received : 19 December 2023
Revised: 5 February 2024
Accepted : 8 February 2024

ABSTRACT

India has a large number of coal deposits, which currently account for 60% of the nation's electricity production. However, burning coal for the purpose of producing energy is not an environmentally friendly practice as it releases large quantities of CO_2 and greenhouse gases into the atmosphere and causes global warming issues. Emissions from power generation plants can be effectively reduced by using an oxy-fuel combustion power generation system with carbon capture and storage. This work presents an effective solution to reduce carbon emissions from coal-powered power plants. The proposed power generation system consists of a coal gasifier integrated with an oxyfuel combustion power cycle and a carbon capture and storage unit. This work discusses three different configurations of coal-based oxy-combustion power generation systems. Each proposed cycles was modelled thermodynamically, and investigations were conducted using the Engineering Equation Solver (EES). The sensitivity analysis and parametric study were performed for the chosen input variables, such as cycle pressure ratio, turbine inlet temperature, coal composition, and split ratio, and observed the effect on net power and thermal efficiency. The results indicate that the coal-based oxyfuel combustion cycles possess high first-law efficiency with a 100% carbon-capturing rate. The thermal efficiency was observed at 23.4% for the basic version of the oxyfuel power cycle. By incorporating a recuperator into the basic cycle, the thermal efficiency reached 39.42%. Further, the recuperator integrated cycle is again modified with stream split and double expansion, and the thermal efficiency of the power cycle reached 41.33%.

Keywords: Oxy Fuel Combustion, Coal Based Power Generation, Emission Free Power Generation, Carbon Capture and Storage, s-CO_2 Power Cycle.

1. Introduction

Coal plays a very important role in the energy sector, as most of the electricity requirements of the sector are fulfilled by coal. As per the study conducted by the National Power Portal of India, 53.25% of total energy capacity is contributed by coal-based thermal power plants [1]. Burning coal for the generation of energy produces a huge amount of carbon dioxide and other greenhouse gases. The emission of these gases into the atmosphere leads to global warming. The consequences of global warming include climate change, temperature rise, water shortages, drought, a shift in rainfall patterns, the melting of ice cover, an accelerating rise in sea level, and species losses. These

* Corresponding author: Meeta Sharma
Amity University Uttar Pradesh, Noida, India-201313
E-mail address: mitu0306@gmail.com

environmental problems directly or indirectly affect mankind, and most of these environmental problems are irreversible in nature, but they can be controlled by reducing greenhouse gas emissions [2].

Reducing carbon emissions from fossil fuel-powered plants is an urgent challenge for the energy-generating industry in order to address global warming and other climate change issues [3]. The most effective technological solution for this issue is carbon capture and storage (CCS) technology. These innovations are capable of capturing carbon dioxide rather than releasing it into the atmosphere. Without damaging the environment, the captured carbon dioxide can subsequently be sent to the geological repository or to storage tanks [4].

There are three principal carbon capture and storage (CCS) technologies: oxy-fuel combustion CCS, post-combustion CCS, and pre-combustion CCS [5]. In pre-combustion CCS, chemical processes are employed to reduce the carbon content of the fuel before combustion [6]. Post-combustion technology recovers carbon from combustion by-products after burning, not prior to its release into the atmosphere [7]. In oxy-combustion technology, the conventional air-fuel combustion mode transitions to a pure oxygen environment. The resulting flue gas, enriched with carbon dioxide and water vapor, is directly utilized for turbine expansion, generating power. The ease of separating carbon dioxide and water at lower pressures and temperatures simplifies the capture process [10].

The oxyfuel power cycle extends its environmental benefits beyond the mere reduction of carbon dioxide emissions. This approach involves burning fuel in an environment enriched with pure oxygen, significantly reducing carbon dioxide emissions and influencing the emission profiles of other pollutants. By minimizing the presence of nitrogen during combustion, the formation of nitrogen oxides (NOx), a common air pollutant, is inherently reduced [38].

Considering the impact on water usage, the oxyfuel power cycle is a critical consideration. Traditional power cycles often demand substantial water resources for cooling, placing significant strain on water supplies. In contrast, the oxyfuel combustion power cycle exhibits considerably lower water demand compared to conventional power plants. A study by Zhu et al. [40] delves into the life cycle water consumption of a 600 MW oxyfuel combustion power plant, finding that, in comparison to traditional power plants, the oxy-combustion CCS power cycle has lower water consumption.

This study focuses on oxyfuel combustion power generation, specifically analyzing the performance of the cycle with various configurations aimed at improving efficiency. The study systematically analyzed three distinct configurations of oxyfuel power cycles, comparing their respective efficiencies. Furthermore, a parametric analysis was conducted to comprehensively assess performance variations. The simulation results are thoroughly compared and discussed in detail in the following sections.

Nomenclature

ASU	Air-separation unit
CCS	Carbon capture and storage
HPT	High pressure turbine
LPT	Low pressure turbine
s-CO_2	Supercritical carbon dioxide
s-H_2O	Supercritical water
LHV	Lower heating value
HHV	Higher heating value
EES	Engineering equation solver
IGCC	Integrated gasification combined cycle
η	Efficiency
γ	Heat capacity ratio
ϵ	Effectiveness
Q	Heat, kW
W	Work, kW
CO_2	Carbon dioxide
H_2O	Water
O_2	Oxygen
H_2	Hydrogen
CH_4	Methane
CO	Carbon monoxide
NO_x	Nitrogen oxides
SO_x	Sulphur oxides
T	Temperature, K
P	Pressure, bar
h	Enthalpy, kJ/kg
s	Entropy, kJ/kgK

2. Literature Review

The key problem for the coal-based thermal power plant is reducing carbon and other environmental emissions while maintaining energy efficiency. The oxy-fuel combustion CCS technology can be

applied as a method to address this issue and reduce greenhouse gas emissions [16]. According to the working fluid, the oxy-combustion power cycles can be broadly divided into two types: supercritical carbon dioxide (s-CO2) cycles and supercritical water (sH2O) cycles. The supercritical carbon dioxide cycles perform better than the supercritical water cycles in the case of coal-based oxy-combustion power cycles [17]. Because of its special qualities, such as its more straightforward carbon capture and storage capabilities and improved energy efficiency, coal-based oxy-fuel combustion s-CO2 power cycles have been the subject of numerous studies.

Allam et al. suggested a coal syngas-fired s-CO2 power cycle with 51.44% net efficiency (LHV) and nearly 100% carbon capture rate. Lu et al [18] conducted a study on the coal variant of this Allam cycle, reviewed the findings and compared it to an IGCC power cycle by including commercially available coal gasifiers. According to the findings, the proposed coal version of the Allam cycle has greater efficiency than an IGCC power cycle without carbon capture and storage. This study also discovered that the efficiency of the power cycle is affected by feedstock choice, gasifier type, and syngas composition.

Weiland et al. conducted research on a coal-fired s-CO2 power plant. The cycle consists of a 300 bar high-pressure oxy combustor, a turbine with a 10:1 pressure ratio, recuperators and heat exchangers, a CO2 capture and storage unit, and a CO2 recirculating loop. According to this study, the oxy-fuel cycle has a net efficiency of 37.7% (HHV), which is 6% higher than the IGCC system, and it produces 13% more net output than the IGCC system even under nearly comparable operating conditions. Weiland et al [21] published a study on the improved s-CO2 coal-based power plant. The improvements in this work include better heat integration and turbine cooling. The changes increase the net efficiency; the observed efficiencies for LHV and HHV are 42.1% and 40.6% respectively.

Zhao et al. [22] conducted a thermodynamic analysis and parametric investigation on the coal gasifier-linked supercritical CO2 power cycle. The parametric study considered turbine intake temperature, inlet pressure, and turbine exit pressure as variables. The research findings highlight the significant influence of turbine intake temperature and expansion pressure (outlet pressure) on the system's net efficiency, while the inlet pressure of the turbine's output has a minor impact. Specifically, when maintaining the turbine input temperature at 1200°C, the suggested cycle demonstrated an impressive 38.88% net efficiency.

Zhao et al. conducted an optimization study on an improved heat integration model. The study employed a two-stage optimization approach, wherein the boundary conditions were initially optimized, followed by the optimization of heat integration procedures. The calculated net efficiency of the primary cycle in this study was 39.5%, while the cycle incorporating a heat integration system demonstrated a higher efficiency of 40.9%. Additionally, the researcher made modifications to the turbine's operating conditions, resulting in a further increase in the cycle's net efficiency, reaching up to 41.41%.

Zhu et al. proposed the Allam-ZC, an innovative coal-based power cycle [23]. This cycle deviates from the conventional Allam cycle through several modifications: 1) Coal gasification employs supercritical steam generated by absorbing heat from the power cycle itself; 2) The back pressure of the turbine is adjusted to a saturated value, eliminating all compressors and retaining only pumps to pressurize the carbon dioxide stream in this cycle; and 3) The turbine exhaust is initially directed through the recuperator before releasing heat. According to the thermodynamic analysis, the Allam-ZC cycle achieves a net efficiency of 47.3% and a carbon dioxide capture rate of 100%.

A solar-hybrid version of the coal oxy-fuel power cycle was modeled by Xu et al. [24]. In this study, the gasification process is heated using concentrated sun energy. The gasification process using solar energy resulted in a 2.9% decrease in coal consumption, and the system has a net efficiency of 43.4% and an energy efficiency of 44.6% without any carbon dioxide emissions from the power plant.

Chen et al. [25] conducted energy and exergy analyses on s-CO2 coal-fired systems incorporating a reheating process. The study examined the impacts of single and double reheat operations. For single and double reheat systems, the research observed energy efficiencies of 48.72% and 49.06%, respectively. The corresponding exergy

efficiencies for these cycles were found to be 47.69% and 48.02%.

3. System Description

This study introduces a coal-based s-CO_2 oxy-combustion power cycle, consisting of four distinct system units: the coal gasification and syngas production unit, air-separation unit, the s-CO_2 power cycle, and the carbon dioxide capture and storage unit. The following section provides a comprehensive description of each component within the system.

3.1. The coal gasification and syngas production unit

The current investigation utilized Indian coal as the fuel input for the power cycle. Table 1 presents the findings of both proximity and ultimate analyses of air-dried Indian coal, sourced from reference [27]. Unlike air steam gasification, this study employed the oxy-steam gasification method. It's important to note that hazardous gases such as sulfur oxides and nitrogen oxides may be present in the coal syngas generated through the gasification process. To address this, a syngas purifier unit is integrated into the gasification and syngas production unit, eliminating these dangerous gases from the syngas before they reach the oxy-fuel combustor. Subsequently, after compression to combustor pressure, the purified syngas is fed into the combustor.

3.2. Air-separation unit (ASU)

In the analysis, a cryogenic air-separation unit (ASU) operating at 30 bar is a consistent component in all proposed cycle models. Following an air filtering procedure to eliminate dust and small airborne particles, the cryogenic ASU intakes fresh air from the atmosphere. To liquefy the air, the filtered air undergoes compression to reach the ASU pressure and is then cooled to a specific cryogenic temperature. Through a technique known as selective distillation, oxygen is extracted from the liquid air, ensuring oxygen purity of 99.5% [28]. The total power required by the ASU unit to separate oxygen and provide 1 kg of oxygen to the combustor is obtained from [29], with power consumption considered as 1080 kJ per kg of oxygen supply.

3.3. The s-CO_2 power cycle

The syngas generated from the coal gasifier unit and the oxygen from the ASU unit are directed to the combustor for oxy-combustion. Oxy-combustion of syngas results in a flue gas rich in carbon dioxide, containing over 95% carbon dioxide, along with water vapor [26]. The resulting combustion products are mixed with the recirculated carbon dioxide stream, and as the carbon dioxide-rich stream expands in the turbine, generates power output.

Following turbine operation, the flue gas is cooled in a gas cooler to reach atmospheric temperature. The key advantage of oxy-combustion technology lies in its straightforward separation and capture of carbon dioxide from the exhaust gas [28]. At atmospheric temperature, carbon dioxide and water vapor in the flue gas are easily separated through water condensation and water separation operations, without involving chemical reactions. Consequently, the energy cost of carbon dioxide separation remains minimal with oxy-combustion technology [16].

After water separation, a series of intercooled compressors increases the pressure of the carbon dioxide stream to a level just above the critical pressure. The surplus carbon dioxide generated during oxy-combustion is then collected and stored in the storage system. Since the carbon dioxide is now above the critical pressure, it exhibits fluid-like properties, facilitating the use of a pump unit to pressurize the carbon dioxide. Through the pump unit, the carbon dioxide stream is pressurized to meet the combustor pressure of the power cycle, and the remaining stream is recirculated within the cycle [30].

Table 1. Analysis of Indian coal [27]

proximate analysis	wt (%)	ultimate analysis	wt (%)
Ash content	36.4	Carbon	43.7
Moisture	5.4	Hydrogen	3.8
Volatiles	28.7	Nitrogen	0.9
Fixed carbon	29.5	Oxygen	14.5
Calorific value=17.76 MJ/kg		Sulphur	0.7

3.4. Carbon capture and storage system

The primary advantage of oxy-combustion technology lies in its straightforward separation and capture of carbon dioxide from exhaust gas [28]. This system employs uncomplicated water condensation and water separation processes, avoiding the need for any chemical reactions to separate water vapor and carbon dioxide in the flue gas. Consequently, with oxy-combustion technology, the energy cost of carbon dioxide separation is minimal [16]. After the removal of carbon dioxide and water from the flue gas, the carbon dioxide stream undergoes supercritical compression in the intercooled compressors. Following compression, any additional CO2 in the recirculated stream is extracted and stored in a carbon dioxide storage system [31].

3.5. Carbon dioxide storage and utilization

Carbon Dioxide Storage involves the consideration of various methods to securely store the captured CO_2. Geological Repositories present a reliable option, where CO_2 is safely stored in deep underground formations. This geological storage offers a secure and permanent solution, preventing the release of CO_2 into the atmosphere. Additionally, Depleted Oil and Gas Reservoirs are recognized as potential storage sites, as injecting CO_2 into these reservoirs not only sequesters the gas but also enhances oil recovery through methods like enhanced oil recovery (EOR) [41].

In Enhanced Oil Recovery (EOR) processes, CO_2 is injected into oil reservoirs to boost oil production, providing economic benefits while simultaneously sequestering CO_2. Furthermore, the utilization of captured CO_2 in various Industrial Processes, such as the production of chemicals, polymers, and fuels, contributes to sustainable practices and reduces reliance on traditional feedstocks. Another innovative approach is carbon mineralization, where CO_2 is reacted with minerals to form stable carbonates. This carbon mineralization not only sequesters CO_2 but also results in the creation of environmentally benign solid products [42].

Considering the Environmental Impact, the storage and utilization of CO_2 emerge as integral components of the proposed power cycles. These strategies ensure a comprehensive approach to addressing climate change. Geological storage, with its secure and long-term solution, complements utilization pathways that contribute to circular economy principles and the creation of value-added products. The combined effort of these storage and utilization measures plays a crucial role in advancing environmental sustainability within the context of proposed power cycles.

4. Proposed Cycle Models

This study introduces and analyses three distinct configurations of coal gasifier-integrated oxy-fuel combustion power cycles. The initial model represents a fundamental oxy-fuel combustion power cycle, the basic cycle (Case-1) is formulated with the essential components. In the second model, the basic coal-based oxy-fuel cycle is enhanced with a recuperator to minimize heat loss (Case-2). The third model (Case-3) is a modification of the second one. In this configuration, following the recuperator heat transfer, the hot recirculated carbon dioxide stream is divided into two parts. The minor stream expands in an additional turbine integrated into the system, while the mainstream is directed straight to the combustion unit.

4.1. Case-1: Basic cycle model

The case-1 model replicates a straightforward coal-based oxy-fuel combustion power cycle utilizing only the essential components. Figure 1 illustrates the process flow diagram for the case-1 cycle. The power plant comprises the gasification and syngas production unit (generating syngas from coal), the air-separation unit (separating oxygen), the sCO2 power cycle (producing power output), and the CO_2 capture and storage unit (capturing and storing carbon dioxide). Descriptions of each of these individual units are provided in the preceding sections.

The oxy-fuel combustor utilizes three inputs: recirculated carbon dioxide, pure oxygen from the air-separation unit, and syngas from the gasifier unit. The resulting flue gas, enriched in carbon dioxide, is generated when the syngas from the gasifier unit combusts in an environment with only pure oxygen. At the outlet of the oxy combustor, the

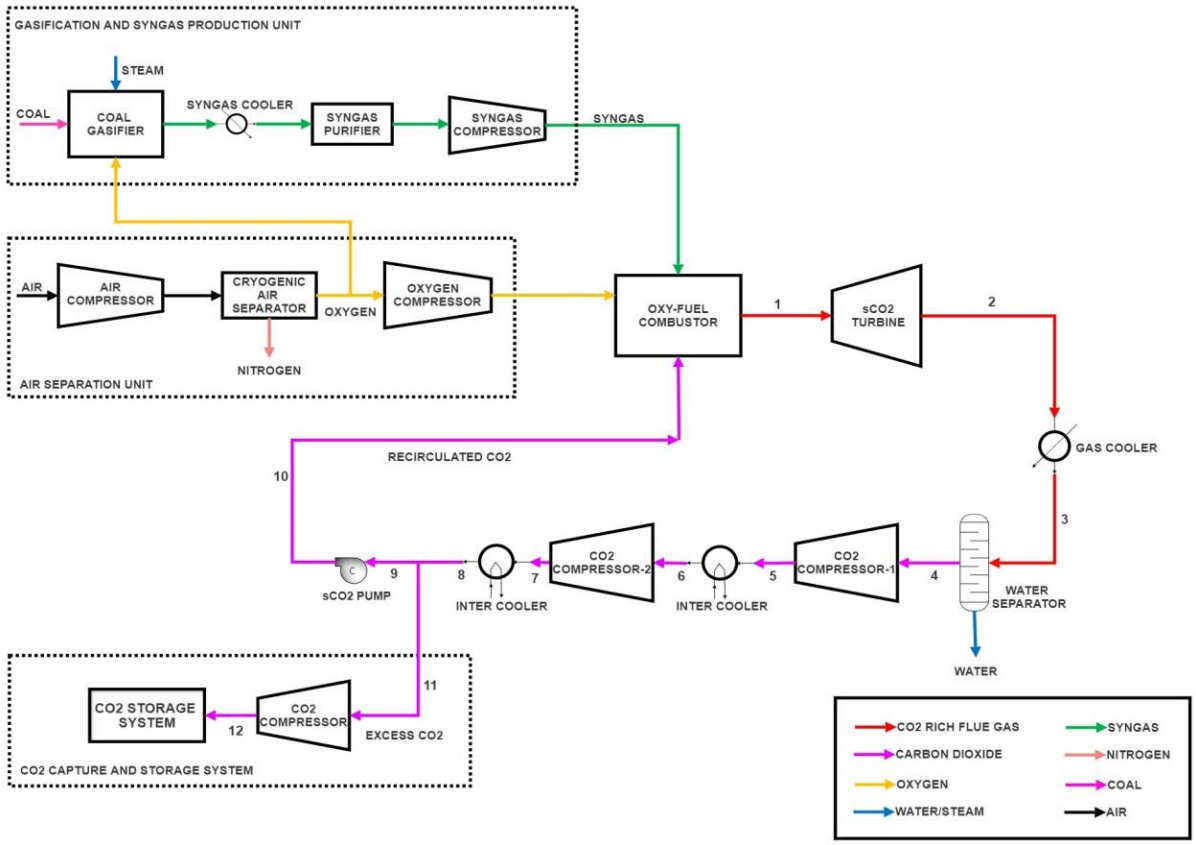

Fig. 1. Case-1: Basic cycle model for the coal-based oxy-fuel combustion power plant.

supercritical flue gas, rich in carbon dioxide, expands in the s-CO_2 turbine, producing power. The expansion process concludes before the flue gas enters the gas cooler, where it is cooled to dissipate heat, causing the steam in the flue gas to condense into water. The water separator then separates the water from the flue gas. After water removal, intercooled two-stage compressors compress the carbon dioxide stream until it reaches a supercritical state. Once the carbon dioxide is compressed to storage pressure, it is extracted from the combustion process and directed to the carbon capture and storage unit. The remaining supercritical CO_2 stream is further compressed to the combustor pressure using a pump.

4.2. Case-2: Recuperator integrated cycle model

The basic cycle model outlined in Case-1 undergoes modification in the Case-2 model. a flue gas cooler is employed to rapidly reduce the temperature of the flue gas from the turbine exhaust to atmospheric levels. To enhance the efficiency of the power cycle, the thermal energy contained in the flue gas, which would otherwise be dissipated into the atmosphere is captured and utilized for regeneration. In the Case-2 model, a recuperator is introduced into the system to recover heat from the turbine exhaust. Figure 2 illustrates the cycle layout with the integrated recuperator. In this configuration, the recuperator serves to transfer heat from the flue gas to the recirculated carbon dioxide stream.

4.3. Case-3: Stream split and double expander cycle model

The case-3 cycle represents a modified version of the case-2 cycle model. After the recuperator absorbs heat, the recirculated carbon dioxide stream in this cycle is split into 10% and 90% streams. The mainstream is directed to the oxy combustor, where it mixes with the flue gas generated by oxy-combustion and undergoes expansion in turbine-1. Simultaneously, the minor stream travels to the gasifier unit, extracting heat from the syngas heat exchanger, undergoing expansion in turbine-2, and then converging with the main stream's exhaust before entering the recuperator. In this model, both turbines operate within a range of 300 bar to 30 bar. The schematic arrangement for the case-3 cycle is depicted in Fig. 3.

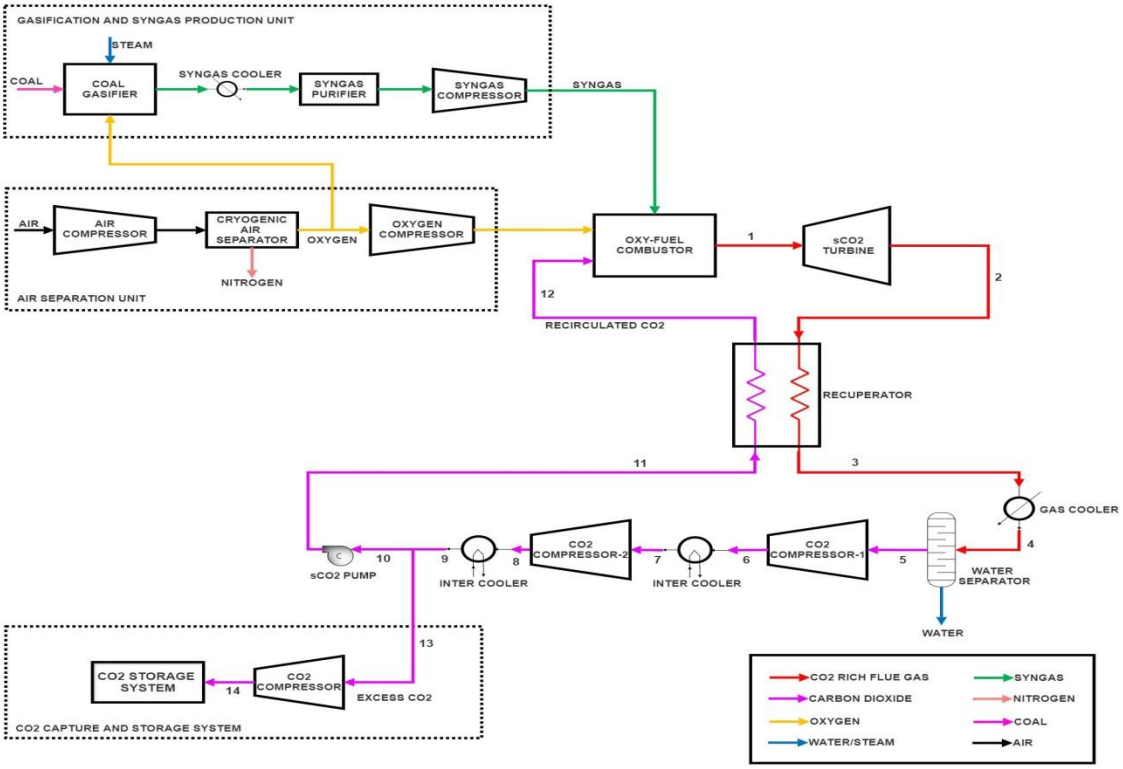

Fig. 2. Case-3: Stream split and double expander cycle model.

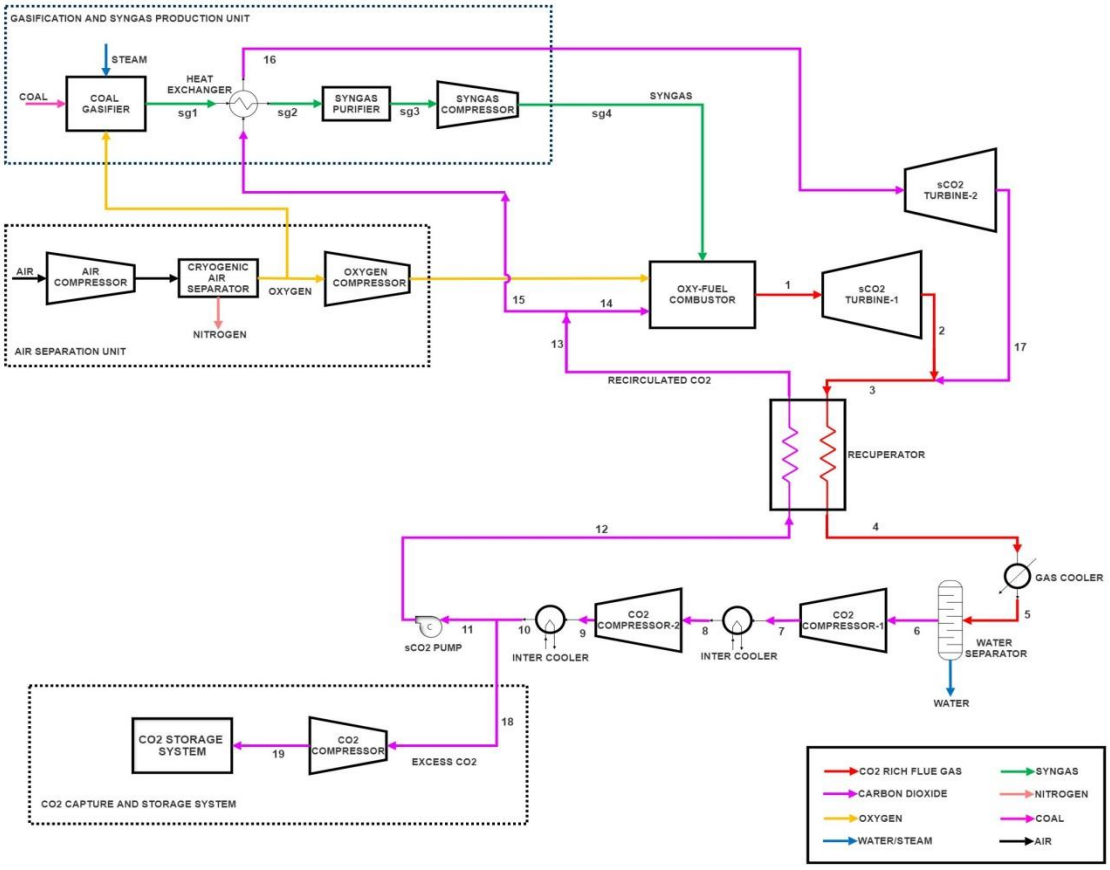

Fig. 3. Case-3: Stream split and double expansion model.

4.4. Assumptions and working parameters

The proposed models in this study are anticipated to yield a net work output of approximately 600MW. As a result, this factor is taken into consideration while choosing the assumptions and operating parameters. Table 2 presents the cycle characteristics and assumptions adopted for this analysis, sourced from references [20], [21], and [22].

5. Mathematical Modelling

The mathematical models for coal gasification and the proposed oxyfuel combustion power cycles are provided below.

5.1. Mathematical model for gasification

The mathematical model for the coal gasification process is explained in this section. The equations are formulated based on the research works detailed in [32], [33], and [34].

The chemical reaction of coal gasification can be written as

$$C_aH_bO_cN_dS_e + fH_2O + gO_2 \rightarrow hCO_2 + iH_2 + jCO + kCH_4 + \frac{d}{2}N_2 + lSO_2 + mH_2O \quad (1)$$

where, a, b, c, d, and e are representing the moles of carbon, hydrogen, oxygen, nitrogen, and sulfur in the coal. Additionally, f and g denote the moles of water vapor and oxygen supplied to the coal gasifier. The moles of CO_2, H_2, CO, CH_4, N_2, SO_2, and H_2O in the syngas are denoted as h, i, j, k, $\frac{d}{2}$, l and m, respectively.

The mass balance of each component in coal and syngas can be written as:

Mass balance of carbon

$$a = h + j + k \quad (2)$$

Mass balance of hydrogen

$$b + 2f = 2i + 4k + 2m \quad (3)$$

Mass balance of oxygen

$$c + f + 2g = 2h + j + 2l + m \quad (4)$$

Mass balance of sulphur

$$e = l \quad (5)$$

The equilibrium constant for the methane formation is

$$K_1 = \frac{k}{i^2} \quad (6)$$

The equilibrium constant for the water gas shift reaction is given by

$$K_2 = \frac{i \times h}{j \times m} \quad (7)$$

where,

$$logK_1 = \frac{466280}{T} - 2.09594 \times 10^{-3} \times T + 0.38620 \times 10^{-6} \times T^2 + 3.034338 \log T - 13.06361 \quad (8)$$

$$logK_2 = \frac{3994.704}{T} - 4.462408 \times 10^{-3} \times T + 0.671814 \times 10^{-6} \times T^2 + 12.220277 \log T - 36.72508 \quad (9)$$

where T is the temperature of the syngas.

The quantities of steam and oxygen supplied to the gasifier units are commonly represented in ratios, specifically the steam-to-carbon ratio and the oxygen-to-carbon ratio. The steam-to-carbon ratio influences methane formation in the syngas, while the oxygen-to-carbon ratio impacts the heating value and gasification efficiency of the system. These ratios are directly obtained from the references.

Table 2. Assumption and working parameters

Parameter	Value
Turbine inlet temperature	1423 K
Turbine inlet pressure	300 bar
Pressure ratio	10
Mass flow rate of working fluid at the turbine inlet	1800 kg/s
Lowest temperature of power cycle	298 K
Compressor outlet pressure	80 bar
Pump outlet pressure	300 bar
Power consumption by the ASU unit	1080 kJ/kg
CO_2 storage pressure	150 bar
Effectiveness of recuperator	0.7
Efficiency of CO_2 turbine	90%
Efficiency of all compressors and pump	85%

The weight of individual components in syngas can be calculated using

$$\text{Weight of individual component of the syngas } w_x = n_x \times m_x \tag{10}$$

where w denotes the weight of the syngas component and the suffix x denotes the individual components in the syngas (CO, H_2O, CO_2, etc.) n denotes the number of moles and m denotes the molar mass of the respective component.

Then the total weight will be given by

$$\text{Total weight} = \sum w_x \tag{11}$$

$$\text{weight percentage of component } x = \frac{w_x}{\text{Total weight}} \tag{12}$$

Then the LHV of the syngas is given by

$$LHV = \sum \text{weight percentage of syngas component } x \times \text{LHV of component } x \text{ in } \frac{kJ}{kg} \tag{13}$$

5.2. Mathematical model for Oxy-fuel combustion

In an oxy-fuel combustor, coal syngas undergoes combustion in a pure oxygen environment, leading to oxy-combustion. This process generates a flue gas composed of carbon dioxide and water vapor. The reactions involved in the oxy-fuel combustion of coal syngas are as follows:

Reaction-1:

$$CO + \frac{1}{2}O_2 \rightarrow CO_2$$

Reaction-2:

$$2H_2 + O_2 \rightarrow 2H_2O$$

Reaction-3:

$$CH_4 + 2O_2 \rightarrow CO_2 + 2H_2O$$

The oxygen requirement, carbon dioxide, and water vapor produced during these reactions can be calculated using the following expressions:

The carbon dioxide formed during the reaction-1:

$$CO_{2\,formed-1} = \frac{\text{Molar mass of carbon dioxide}}{\text{Molar mass of carbon monoxide}} \times wt\%\ of\ CO \times m_{fuel} \tag{14}$$

The oxygen required for reaction -1:

$$O_{2required-1} = \frac{\frac{1}{2}\,\text{Molar mass of oxygen}}{\text{Molar mass of carbon monoxide}} \times wt\%\ of\ CO \times m_{fuel} \tag{15}$$

The water vapor formed during reaction-2:

$$H_2O_{formed-2} = \frac{2 \times \text{Molar mass of water}}{2 \times \text{Molar mass of hydrogen}} \times wt\%\ of\ H_2 \times m_{fuel} \tag{16}$$

The oxygen required for the reaction-2:

$$O_{2required-2} = \frac{\text{Molar mass of oxygen}}{2 \times \text{Molar mass of hydrogen}} \times wt\%\ of\ H_2 \times m_{fuel} \tag{17}$$

The carbon dioxide during the reaction -3

$$CO_{2\,formed-3} = \frac{\text{Molar mass of carbon dioxide}}{\text{Molar mass of methane}} \times wt\%\ of\ CH_4 \times m_{fuel} \tag{18}$$

The water vapor during the reaction -3:

$$H_2O_{formed-3} = \frac{2 \times \text{Molar mass of water}}{\text{Molar mass of methane}} \times wt\%\ of\ CH_4 \times m_{fuel} \tag{19}$$

The oxygen required for the reaction-3:

$$O_{2required-3} = \frac{\text{Molar mass of oxygen}}{\text{Molar mass of methane}} \times wt\%\ of\ CH_4 \times m_{fuel} \tag{20}$$

Then, The total carbon dioxide formed during the oxy-fuel combustion is:

$$\text{Total } CO_2 \text{ formed} = CO_{2\,formed-1} + CO_{2\,formed-3} + wt\%\ of\ CO_2 \times m_{fuel} \tag{21}$$

Total water vapor formed during the oxy-fuel combustion is:

$$\text{Total } H_2O \text{ formed} = H_2O_{formed-2} + H_2O_{formed-3} + wt\%\ of\ H_2O \times m_{fuel} \tag{22}$$

The total oxygen required for oxy-fuel combustion is calculated using the following equation, and a 3% excess oxygen supply is considered to the combustor to ensure proper syngas combustion:

$$\text{Total } O_2 \text{ required} = O_{2required-1} + O_{2required-2} + O_{2required-3} + 0.03 \times \left(O_{2required-1} + O_{2required-2} + O_{2required-3}\right) \tag{23}$$

5.3. Mathematical models based on laws of thermodynamics

5.3.1. Mathematical model for case-1

The mathematical model for the case-1 cycle is shown in Table 3.

Table 3. Mathematical model for case-1

Items	Calculation formula	No.
Isentropic temperature at outlet of turbine	$T_{isentropic\ out} = \frac{T_{in}}{Pressure\ ratio^{\frac{\gamma-1}{\gamma}}}$	(24)
Actual temperature at outlet of turbine	$T_{out} = T_{in} - (T_{in} - T_{isentropic\ out}) \times \eta_{isentropic\ turbine}$	(25)
Work output of the turbine	$W_{turbine} = m_{in} \times (h_{in} - h_{out})$	(26)
Heat released in gas cooler	$Q_{Released} = m_{in} \times (h_{in} - h_{out})$	(27)
Water content removed in water cooler	$m_{water\ removed} = Total\ H_2O\ formed\ during\ combustion$	(28)
Mass of carbon dioxide at outlet of the water separator	$m_{CO2\ out} = m_{in} - m_{water\ removed}$	(29)
Isentropic temperature at outlet of the compressor or pump	$T_{isentropic\ out} = T_{in} \times \frac{P_{out}}{P_{in}}^{\frac{\gamma-1}{\gamma}}$	(30)
Actual temperature at outlet of the compressor or pump	$T_{out} = T_{in} + \frac{T_{isentropic} - T_{in}}{\eta_{compressor}}$	(31)
Work required for the compressor or pump	$W_{compressor\ or\ pump} = m_{co2\ out} \times (h_{out} - h_{in})$	(32)
Heat transfer in intercooler	$Q_{inter\ cooler} = m_{co2\ out} \times (h_{in} - h_{out})$	(33)
Mass of carbon dioxide captured	$m_{CO_2\ captured} = Total\ CO_2\ formed\ during\ combustion$	(34)
Mass of carbon dioxide recirculated	$m_{recirculated} = m_{co2\ out} - m_{CO2\ captured}$	(35)
Power consumption by ASU unit	$ASU\ power\ consumption = Total\ O_2\ required \times the\ energy\ consumption\ by\ ASU\ unit\ to\ supply\ 1kg\ of\ O_2$	(36)
The network output of the power cycle	$W_{net} = W_{turbine} - (\Sigma\ W_{compressors\ and\ pump} + ASU\ power\ consumption)$	(37)
Heat input to the system	$Q_{in} = m_{fuel} \times LHV$	(38)
Net efficiency the power cycle	$\eta_{net} = \frac{W_{net}}{Q_{in}}$	(39)

5.3.2. Mathematical model for case-2

In this case, a recuperator device is introduced into the system, in addition to case-1, to recover heat from the flue gas. Table 4 provides a detailed mathematical model for the recuperation process. The descriptions of all other mathematical equations necessary to describe the processes covered in the case-2 model remain the same as in the case-1 model.

5.3.3. Mathematical model for case-3

As discussed in the previous sections, the case-3 cycle is a modified version of the case-2 cycle. The modifications include stream splitting and additional turbine expansion. The mathematical equations required to model the case-3 cycle, in addition to the case-2 cycle, are presented in Table 5.

Table 4. Mathematical model for case-2.

Items	Calculation formula	No.
Maximum heat transfer in recuperator	$Q_{max} = C_{min} \times (T_2 - T_{11})$	(40)
Actual heat transfer in recuperator	$Q_{recuperate} = Q_{max} \times \epsilon$	(41)
Temperature of flue gas at outlet of the recuperator	$T_{fluegas\ out} = T_{flue\ gas\ in} - \frac{Q_{recuperator}}{m_{flue\ gas} cp_{flue\ gas}}$	(42)
Temperature of recirculated CO_2 at outlet of the recuperator	$T_{recirculated\ CO2\ out} = T_{recirculated\ CO2\ out} + \frac{Q_{recuperator}}{m_{recirculated\ CO2} cp_{recirculated\ CO2}}$	(43)

Table 5. Mathematical model for case-3.

Items	Calculation formula	No.
Mass flow of carbon dioxide to turbine-2	$m_{CO2\ to\ turbine-2} = stream\ split\ percentage \times m_{recirculated\ CO2}$	(44)
Mass flow of carbon dioxide to oxy combustor	$m_{CO2\ to\ oxy\ combustor} = (1 - stream\ split\ percentage) \times m_{recirculated\ CO2}$	(45)
Maximum heat transfer in heat exchanger	$Q_{\max hx} = C_{min} \times (T_{sg} - T_2)$	(46)
Actual heat transfer in heat exchanger	$Q_{addition} = Q_{\max hx} \times \varepsilon$	(47)
Temperature of flue gas at outlet of the heat exchanger	$T_{flue\ gas\ at\ outlet\ of\ hx} = T_{flue\ gas\ at\ inlet\ of\ hx} + \frac{Q_{addition}}{m_2 cp_2}$	(48)
The net work output of the power cycle	$W_{net} = \Sigma\, W_{turbine} - (\Sigma\, W_{compressors\ and\ pump} + ASU\ power\ consumption)$	(49)

6. Results and Observations

The proposed emission-free power cycles were the subject of thermodynamic analyses, and the outcomes of the thermodynamic simulations are discussed below.

6.1. Coal gasification and syngas composition

This section presents the simulation results for the coal gasification process. The gasification efficiency for the coal gasifier, determined through thermodynamic calculations, is 62.04%, and the Lower Heating Value (LHV) for coal syngas, also determined by thermodynamic calculations, is 10.9 MJ/kg. Table 6 illustrates the syngas compositions as determined in the study.

The study found that the oxygen to carbon ratio (mol/mol) affects the LHV and the composition of the syngas. Table 6 illustrates the variation in LHV and volumetric percentages of syngas compositions concerning the oxygen-to-carbon ratio. According to the graphical data, it is evident that the volume percentages of carbon dioxide and water vapor increase as the oxygen-to-coal ratio rises. Conversely, the percentages of carbon monoxide and hydrogen decrease significantly with an increase in the oxygen-to-coal ratio. These fluctuations result from increased coal combustion due to an abundance of oxygen, leading to a reduction in the proportion of carbon monoxide and hydrogen in syngas, consequently affecting the LHV.

Table 6. Results obtained by coal gasification.

ELEMENT	Vol %
CO	57.06
H_2	38.59
CH_4	0.6
CO_2	0.3
H_2O	2.6
N_2	0.52
SO_2	0.35

LHV=10.9 MJ/kg
Gasification efficiency= 62.04

6.2. Performance of proposed cycles

6.2.1. Case-1: Basic cycle

The mathematical model for the case-1 cycle is implemented and simulated using EES software for thermodynamic analysis. The results of the simulation, as depicted in Table 7, reveal that the first law efficiency of the basic cycle is approximately 23.4%. The basic cycle generates a net power output of 595.6 MW, utilizing 132.9 kg/s of coal to produce power and capturing carbon dioxide at a rate of 422.6 kg/s. The outcomes highlight the relatively low net efficiency of the case-1 cycle, indicating the potential for improvement through the application of heat integration strategies in conjunction with the basic cycle.

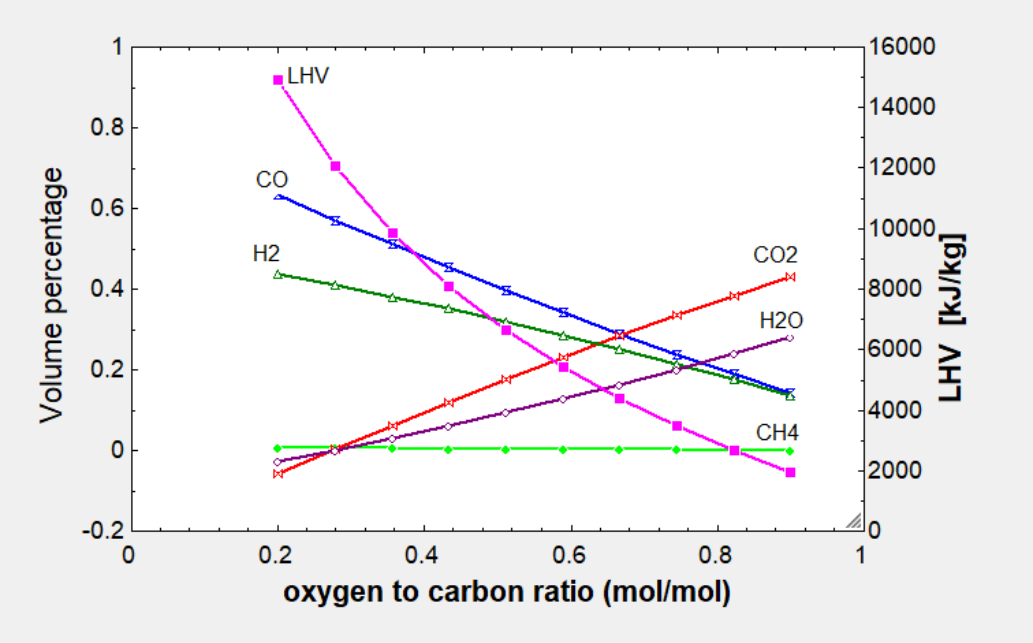

Fig. 4. Oxygen to carbon ratio vs volumetric composition and LHV.

Table 7. Simulation results of case-1.

Item	Value	Unit
Net work output	595.6	MW
Heat input	2547	MW
Net efficiency	23.4	%
Coal consumption	132.9	kg/s
Water removal rate	107.4	kg/s
Carbon dioxide capturing rate	422.6	kg/s
ASU power consumption	263.8	MW

6.2.2. Case-2: Recuperator integrated power cycle

The case-2 cycle, a modified version of the case-1 cycle, incorporates a recuperator to address heat loss issues observed in the case-1 cycle. Utilizing EES software, a thermodynamic analysis of this recuperator-integrated power cycle is conducted, and the results are presented in Table 8. The thermodynamic simulation reveals improved performance in the case-2 cycle compared to the case-1 cycle. The incorporation of the recuperator significantly reduces the heat required for the power cycle, leading to enhanced thermodynamic efficiencies, reaching 39.42%. Consequently, the required heat input decreases, resulting in reduced coal consumption, syngas burn rate, and carbon dioxide production during oxy-combustion. The carbon-capturing rate for the case-2 cycle is measured at 286.3 kg/s.

6.2.3. Case-3: Stream split and double expander cycle model

The case-3 cycle, featuring stream split and double expansion, is analyzed through thermodynamic simulation, and the results are presented in Table 9. The incorporation of stream split and double expansion enhances the net efficiency by 1.91% compared to case-2. In this configuration, the net efficiency reaches 41.33%, generating a net output of 752.76 MW, with a carbon-capturing rate of 302.3 kg/s. This cycle demonstrates superior thermodynamic performance compared to the other two cases.

6.3. Parametric analysis

The identification of critical parameters influencing system performance is facilitated by parametric studies, which are crucial for understanding system behavior. This section delves into the major variables that impact the performance of coal-powered oxy-fuel combustion power cycles.

Table 8. Simulation results of case-2.

Item	Value	Unit
Net work output	669.36	MW
Heat input	1698	MW
Net efficiency	39.42	%
Coal consumption	88.64	kg/s
Water removal rate	73.65	kg/s
Carbon dioxide capturing rate	286.3	kg/s
ASU power consumption	175.98	MW

Table 9. Simulation results of case-3.

Item	Value	Unit
Net work output	752.76	MW
Heat input	1821	MW
Net efficiency	41.33	%
Coal consumption	95.08	kg/s
Water removal rate	76.83	kg/s
Carbon dioxide capturing rate	302.3	kg/s
ASU power consumption	188.77	MW

6.3.1. Effect of inlet temperature

In Fig. 5, the impact of varying the turbine inlet temperature (TIT) is illustrated along with its net efficiency(η_{net}), second law efficiency($\eta_{second\ law}$), net work output(W_{net}), and required heat input(Q_{in}). Throughout this investigation, the turbine inlet pressure is maintained at 300 bar, while the inlet temperature is adjusted between 1073K and 1973K. Upon analysis, it is evident that the slope of the heat input curve is somewhat steeper than that of the net work output curve. Both net work output and required heat input exhibit nearly linear growth with an increase in turbine inlet temperature. Net efficiency and second law efficiency experience significant improvements with the rise in turbine inlet temperature up to 1400K. Beyond this point, the impact on efficiencies becomes minimal, and they remain relatively constant. Similar observations were drawn from parametric studies conducted by Weiland et al. [20] and Scaccaborazzi et al. [37].

6.3.2. Effect of pressure ratio

In Fig. 6, the impact of pressure ratio on net efficiency (ηnet) is depicted. the analysis reveals the following key observations: the net efficiency of the cycle is notably low when the pressure ratio is below 5. Significant improvements in net efficiency occur with an increase in the pressure ratio from 5 to 12. However, further increases in pressure ratio beyond 12 have minimal impact on net efficiency, and the net efficiency remains nearly constant.

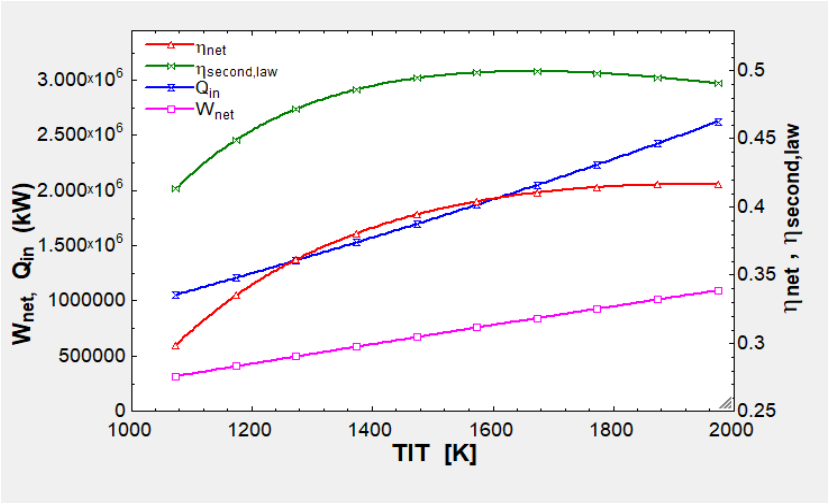

Fig. 5. Effect of turbine inlet temperature

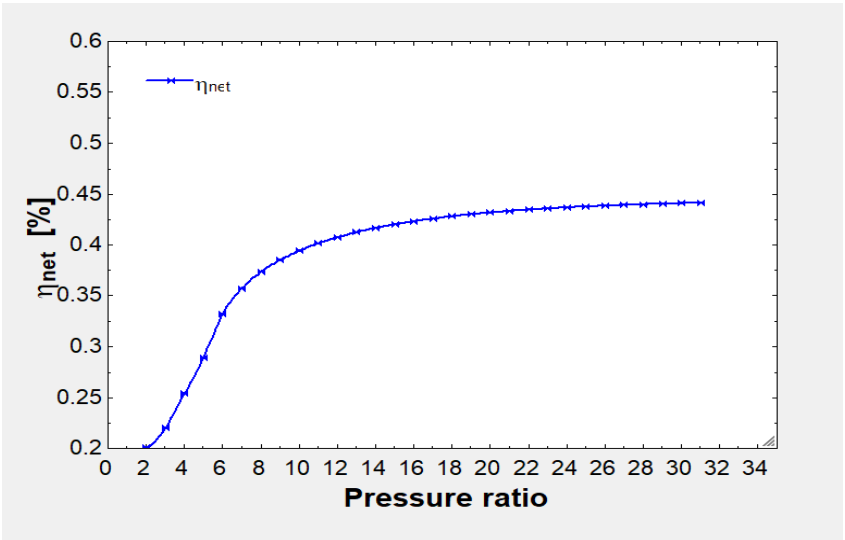

Fig. 6. Effect of pressure ratio.

6.3.3. Effect of recuperator heat transfer

The investigation into the impact of recuperator heat transfer (Qrecup) is presented in Fig. 7, along with the corresponding graphical results. The recuperator heat transfer rate is varied from the minimum achievable value to the maximum rate. The findings show that an increase in the recuperator heat transfer rate reduces the required heat input (Qin) for the system, leading to an improvement in the net efficiency of the power cycle. This study suggests that even a slight increase in the recuperator heat transfer rate can significantly enhance the overall efficiency of the power plant.

6.3.4. Effect of stream split percentage

In the parametric investigation using the case-3 cycle, the impact of the stream split percentage on power cycle net efficiency is explored, and the results are depicted in Fig. 8. The findings indicate that increasing the stream split percentage up to 20% enhances the net efficiency of the cycle. However, a further increase in the stream split percentage leads to a reduction in net efficiency. This decrease is attributed to the fact that an increased stream split reduces the flow of recirculated carbon dioxide to the combustor, influencing the mass and energy flow of the flue gas through the turbine unit, resulting in lower net output and net efficiency.

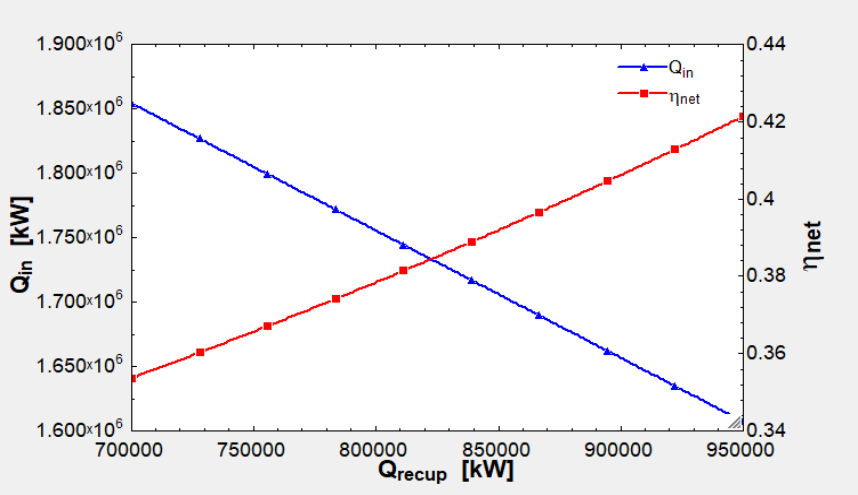

Fig. 7. Effect of recuperator heat transfer.

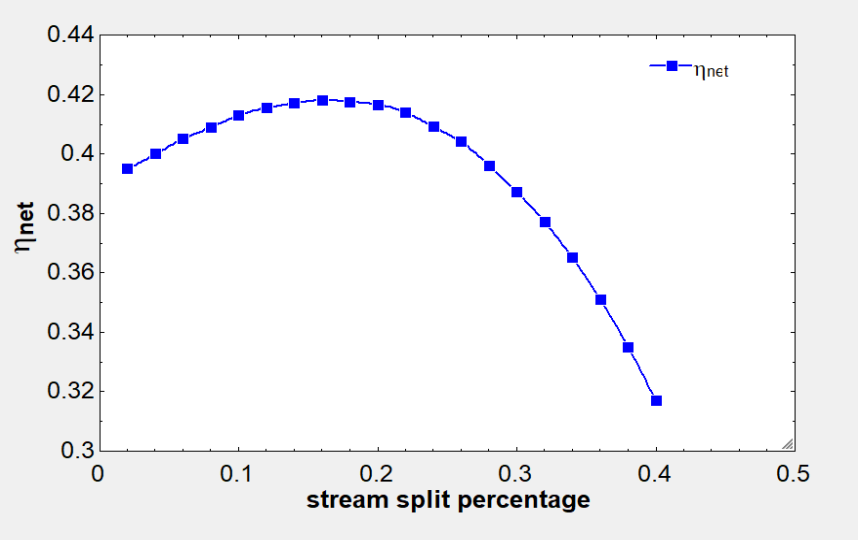

Fig. 8. Effect of stream split percentage.

7. Techno economic feasibility of oxy fuel combustion power plants

This study proposes an oxy-fuel combustion cycle with carbon capture as a viable solution to reduce carbon dioxide emissions from power plants. This section discusses the literature survey conducted to assess the techno-economic feasibility of oxy-combustion power cycles.

Cormos et.al [43] assessed a coal-based supercritical oxy-combustion power plant, indicated that the specific capital investment was lower than gas–liquid alternatives (2285 €/kW net power compared to 2500 €/kW net power), and the study states that oxy-fuel combustion power plants fuelled by coal, lignite, and sawdust. The findings indicated that the proposed process would incur efficiency penalties ranging from 9-12% points compared to a reference coal-fired power plant lacking Carbon Capture and Storage (CCS). The primary challenge associated with oxy-fuel combustion stems from the substantial efficiency penalties arising from high-purity O2 production in the air-separation unit (ASU) (50-60%) and CO_2 compression in the Carbon Capture Unit (CPU) (30-40%), collectively contributing to about 90% of the energy penalty [44]. Consequently, this leads to a 50–95% increase in the Levelized Cost of Electricity (LCOE). Singh et al. [45] conducted a comparative analysis of the techno-economic performance of amine scrubbing and oxy-fuel combustion retrofitted into an existing coal-fired power plant. Both processes were found to elevate electricity prices by 20–30% when compared to the reference coal-fired power plant without CCS. However, oxy-fuel combustion emerged as a more appealing option due to its lower CO_2 emissions and a reduced cost of CO_2 capture. Literature reports suggest that the LCOE of oxy-coal combustion using coal falls between 70 €/MWelh [43] and 106.3 €/MWelh [46], while utilizing sawdust results in 78.87 €/MWelh [43]. Consequently, it is imperative to explore options for minimizing the energy demand of oxy-fuel combustion and enhancing its economic viability for scalable deployment. Zhou et al. [47] proposed an integrated Chemical Looping Air-Separation Unit (ICLAS) to tackle the high-power demand of the cryogenic-based ASU. Their study demonstrated that ICLAS, utilizing steam and recycled flue gas, significantly improved the techno-economic performance of the oxy-fuel combustion power plant. Moreover, the application of ICLAS was shown to reduce the efficiency penalty of oxy-fuel combustion from 9.5% to 5% and potentially lower the LCOE by up to 20%. Xiaoyu et al. [48] conducted a techno-economic assessment on oxy fuel combustion power cycles. The outcomes revealed that substituting the conventional oxy-fuel steam cycle with the supercritical carbon dioxide cycle resulted in a decrease in efficiency penalties by up to 2% points, along with a reduction in the levelized cost of electricity by up to 4.6% (4.1 €/MWh). Conversely, when biomass was employed as a fuel, there was an increase in net efficiency penalties by 0.5% points, and the levelized cost of electricity experienced a rise of 24.4 €/MWh.

8. Comparison and validation

Comparison of simulation results with other similar research works are shown in Table 10. Zhao et al. [22] reported a net efficiency of 38.21% and a net work output of 534.98MW for a coal-based direct-fired s-CO_2 power cycle. Wieland et al. [38] found a net efficiency of 40.6% and a net work output of 606MW for an oxy-fuel combustion power cycle. The case-2 cycle model in this study achieved a net efficiency of 39.42% and a net work output of 669.39MW, while the updated case-3 cycle model achieved a net efficiency of 41.33% and a net work output of 752.76MW. Slight variations in net efficiency and net output values between the proposed cycles and reference studies may be attributed to differences in assumptions, selected coal types, and other simulation parameters. Additionally, the findings of this study are compared to an Integrated Gasification Combined Cycle (IGCC) system with carbon capture and storage [39]. In this comparison, the oxy-fuel combustion power cycles demonstrate higher thermodynamic efficiency than the IGCC system with carbon capture and storage.

Table 10. Comparison of proposed cycles performance with similar research works

Item	Recuperative s-CO_2 power cycle (Case-2)	Stream split version of s-CO_2 power cycle (Case-3)	Coal based direct-fired s-CO_2 power cycle [22]	Gasifier integrated direct fired s-CO_2 power cycle [38]	IGCC with carbon capture and storage [39]
Coal type	Indian coal	Indian coal	Illinois #6	Illinois #6	Illinois #6
Cycle medium	CO_2 rich flue gas	CO_2 rich flue gas	CO_2 rich flue gas	CO_2 rich flue gas	AHT+ Steam
Turbine inlet temperature (℃)	1200	1200	1200	1200	1450
Net power output (MW)	669.36	752.76	534.98	606	771
Net plant efficiency (%)	39.42	41.33	38.21	40.6	35.7
Carbon capture %	~100	~100	~100	99.8	99.5

9. Conclusions

This study encompassed both energy and parametric analyses, exploring various configurations of coal-based oxy-fuel combustion power cycles. The following section outlines the conclusions derived from this investigative study.

- According to the investigation, the coal version of the oxy-fuel combustion power cycle is a preferred and promising technology for generating electricity without emitting any carbon dioxide into the atmosphere. The analysis found that the proposed power cycles have an excellent net efficiency.
- This investigation delved into the thermodynamics of three alternative configurations of coal-based oxy-combustion power cycles. The thermodynamic analysis of the basic cycle model presented in Case-1 yielded a net efficiency of 23.4%. Compared to other power cycles based on the Brayton cycle, the efficiency obtained for the Case-1 cycle is relatively low. The net efficiency of the power cycle was elevated to 39.42% by enhancing the basic cycle model through the integration of a recuperator with the system for regeneration purposes, as outlined in Case-2. A modified cycle, as detailed in Case-3, involving a stream split and a double expander, increased the net efficiency of the power cycle to 41.33%. This represents the highest efficiency observed throughout this investigation.
- The results obtained from the parametric analysis are as follows:
- The coal-based oxy-combustion power cycle exhibits better cycle performance when the turbine inlet temperature is above 1400 K, and the value of the pressure ratio is between 5 to 12.
- The recuperative heat transfer rate has a significant impact on net efficiency. A slight enhancement in the heat transfer rate improves the thermodynamic performance of the power cycle.
- For the Case-3 power cycle, increasing the stream split percentage by up to 20% enhances the net efficiency. However, further increasing the percentage of stream split beyond 20% diminishes the net efficiency of the power cycle.

According to the comparative analysis, the oxy-fuel combustion power cycles proposed in Case-3 (stream split and double expander cycle model) are more energy-efficient than the IGCC system with carbon capture and storage. The net efficiency of the proposed cycles is 41.33%, approximately 5% higher than the IGCC system.

References

[1] Location wise regional summary of all India installed capacity (IN MW) of power stations as on 31/12/2020" (PDF). National Power Portal, GoI. Retrieved 19 January 2021.

[2] Fletcher WD, Smith CB. Reaching net zero: What it takes to solve the global climate crisis: Elsevier; 2020.

[3] Zachary J. Options for reducing a coal-fired plant's carbon footprint, Part II. Power (New York). 2008;152(7).
[4] Rackley S. Carbon capture and storage: Butterworth-Heinemann Press; 2017.
[5] Omoregbe O, Mustapha AN, Steinberger-Wilckens R, El-Kharouf A, Onyeaka H. Carbon capture technologies for climate change mitigation: A bibliometric analysis of the scientific discourse during 1998–2018. Energy reports. 2020;6:1200-12.
[6] Suomalainen MS, Arasto A, Teir S, Siitonen S. Improving a pre-combustion CCS concept in gas turbine combined cycle for CHP production. Energy Procedia. 2013;37:2327-40.
[7] Wang J-J, Jing Y-Y, Zhang C-F, Zhao J-H. Review on multi-criteria decision analysis aid in sustainable energy decision-making. Renewable and sustainable energy reviews. 2009;13(9):2263-78.
[8] Goanta A, Bohn J-P, Blume M, Li X, Spliethoff H, editors. Numerical Characterization of a Novel Staged Combustion Concept Applied to Oxy-Fuel Carbon Capture Technology. ASME International Mechanical Engineering Congress and Exposition; 2011.
[9] Vasudevan S, Farooq S, Karimi IA, Saeys M, Quah MC, Agrawal R. Energy penalty estimates for CO2 capture: Comparison between fuel types and capture-combustion modes. Energy. 2016;103:709-14.
[10] Chen S, Zheng Y, Wu M, Hu J, Xiang W. Thermodynamic analysis of oxy-fuel combustion integrated with the sCO2 Brayton cycle for combined heat and power production. Energy Conversion and Management. 2021;232:113869.
[11] Zhang Z, Li X, Luo C, Zhang L, Xu Y, Wu Y, et al. Investigation on the thermodynamic calculation of a 35 MWth oxy-fuel combustion coal-fired boiler. International Journal of Greenhouse Gas Control. 2018;71:36-45.
[12] Scheffknecht G, Al-Makhadmeh L, Schnell U, Maier J. Oxy-fuel coal combustion—A review of the current state-of-the-art. International Journal of Greenhouse Gas Control. 2011;5:S16-S35.
[13] Wall T, Yu J, editors. Coal-fired oxyfuel technology status and progress to deployment. The Proceedings of the 35th International Technical Conference on Clean Coal & Fuel Systems, The Clearwater Clean Coal Conference June; 2009.
[14] Buhre BJ, Elliott LK, Sheng C, Gupta RP, Wall TF. Oxy-fuel combustion technology for coal-fired power generation. Progress in energy and combustion science. 2005;31(4):283-307.
[15] Skorek-Osikowska A, Bartela L, Kotowicz J, Job M. Thermodynamic and economic analysis of the different variants of a coal-fired, 460 MW power plant using oxy-combustion technology. Energy Conversion and management. 2013;76:109-20.
[16] Rogalev N, Petrenya YK, Kindra V, Rogalev A. Oxy-fuel power cycles promoting the transition to green and sustainable future in the energy sector. Sustainable Fuel Technologies Handbook: Elsevier; 2021. p. 513-39.
[17] Crespi F, Gavagnin G, Sánchez D, Martínez GS. Supercritical carbon dioxide cycles for power generation: A review. Applied energy. 2017;195:152-83.
[18] Lu X, Forrest B, Martin S, Fetvedt J, McGroddy M, Freed D, editors. Integration and optimization of coal gasification systems with a near-zero emissions supercritical carbon dioxide power cycle. Turbo Expo: Power for Land, Sea, and Air; 2016: American Society of Mechanical Engineers.
[19] Allam R, Fetvedt J, Forrest B, Freed D, editors. The oxy-fuel, supercritical CO2 Allam Cycle: New cycle developments to produce even lower-cost electricity from fossil fuels without atmospheric emissions. Turbo Expo: Power for Land, Sea, and Air; 2014: American Society of Mechanical Engineers.
[20] Shelton W, White C, Gray D, Weiland N. Performance baseline for direct-fired sCO2 cycles. National Energy Technology Laboratory (NETL), Pittsburgh, PA, Morgantown, WV …; 2016.
[21] Weiland NT, White CW. Techno-economic analysis of an integrated gasification direct-fired supercritical CO2 power cycle. Fuel. 2018;212:613-25.
[22] Zhao Y, Wang B, Chi J, Xiao Y. Parametric study of a direct-fired

supercritical carbon dioxide power cycle coupled to coal gasification process. Energy conversion and management. 2018;156:733-45.

[23] Zhu Z, Chen Y, Wu J, Zheng S, Zhao W. Performance study on s-CO2 power cycle with oxygen fired fuel of s-water gasification of coal. Energy Conversion and Management. 2019;199:112058.

[24] Xu C, Xin T, Li X, Li S, Sun Y, Liu W, et al. A thermodynamic analysis of a solar hybrid coal-based direct-fired supercritical carbon dioxide power cycle. Energy conversion and management. 2019;196:77-91.

[25] Chen Z, Wang Y, Zhang X. Energy and exergy analyses of S–CO2 coal-fired power plant with reheating processes. Energy. 2020;211:118651.

[26] Zhang Y, Li H, Han W, Bai W, Yang Y, Yao M, et al. Improved design of supercritical CO2 Brayton cycle for coal-fired power plant. Energy. 2018;155:1-14.

[27] Kumar KV, Bharath M, Raghavan V, Prasad B, Chakravarthy S, Sundararajan T. Gasification of high-ash Indian coal in bubbling fluidized bed using air and steam–An experimental study. Applied Thermal Engineering. 2017;116:372-81.

[28] Jin B, Zhao H, Zheng C, Liang Z. Control optimization to achieve energy-efficient operation of the air separation unit in oxy-fuel combustion power plants. Energy. 2018;152:313-21.

[29] Thorbergsson E, Grönstedt T. A Thermodynamic Analysis of Two Competing Mid-Sized Oxyfuel Combustion Combined Cycles. Journal of Energy. 2016; 2016(1):2438431.

[30] Zhao Y, Yu B, Wang B, Zhang S, Xiao Y. Heat integration and optimization of direct-fired supercritical CO2 power cycle coupled to coal gasification process. Applied Thermal Engineering. 2018;130:1022-32.

[31] Cormos C-C. Oxy-combustion of coal, lignite and biomass: A techno-economic analysis for a large scale Carbon Capture and Storage (CCS) project in Romania. Fuel. 2016;169:50-7.

[32] Żogała A. Equilibrium simulations of coal gasification–factors affecting syngas composition. Journal of Sustainable Mining. 2014;13(2):30-8.

[33] La Villetta M, Costa M, Massarotti N. Modelling approaches to biomass gasification: A review with emphasis on the stoichiometric method. Renewable and Sustainable Energy Reviews. 2017;74:71-88.

[34] Zainal Z, Ali R, Lean C, Seetharamu K. Prediction of performance of a downdraft gasifier using equilibrium modeling for different biomass materials. Energy conversion and management. 2001;42(12):1499-515.

[35] Sleiti AK, Al-Ammari WA. Energy and exergy analyses of novel supercritical CO2 Brayton cycles driven by direct oxy-fuel combustor. Fuel. 2021;294:120557.

[36] Luo J, Emelogu O, Morosuk T, Tsatsaronis G. Exergy-based investigation of a coal-fired allam cycle. Energy. 2021;218:119471.

[37] Scaccabarozzi R, Gatti M, Martelli E. Thermodynamic analysis and numerical optimization of the NET Power oxy-combustion cycle. Applied energy. 2016;178:505-26.

[38] Shelton WW, Ames RW, Dennis RA, White CW, Plunkett JE, Fisher JC, et al., editors. Advanced and Transformational Hydrogen Turbines for Integrated Gasification Combined Cycles. Turbo Expo: Power for Land, Sea, and Air; 2016: American Society of Mechanical Engineers.

[39] Zhu Y, Chen M, Yang Q, Alshwaikh MJ, Zhou H, Li J, et al. Life cycle water consumption for oxyfuel combustion power generation with carbon capture and storage. Journal of Cleaner Production. 2021;281:124419.

[40] Gür TM. Carbon dioxide emissions, capture, storage and utilization: Review of materials, processes and technologies. Progress in Energy and Combustion Science. 2022;89:100965.

[41] Zhang Z, Pan S-Y, Li H, Cai J, Olabi AG, Anthony EJ, et al. Recent advances in carbon dioxide utilization. Renewable and sustainable energy reviews. 2020;125:109799.

[42] Hanak DP, Powell D, Manovic V. Techno-economic analysis of oxy-

combustion coal-fired power plant with cryogenic oxygen storage. Applied Energy. 2017;191:193-203.

[43] Singh D, Croiset E, Douglas PL, Douglas MA. Techno-economic study of CO2 capture from an existing coal-fired power plant: MEA scrubbing vs. O2/CO2 recycle combustion. Energy conversion and Management. 2003;44(19):3073-91.

[44] Tola V, Cau G, Ferrara F, Pettinau A. CO2 emissions reduction from coal-fired power generation: A techno-economic comparison. Journal of Energy Resources Technology. 2016;138(6):061602.

[45] Zhou C, Shah K, Moghtaderi B. Techno-economic assessment of integrated chemical looping air separation for oxy-fuel combustion: an Australian case study. Energy & Fuels. 2015;29(4):2074-88.

[46] Wei X, Manovic V, Hanak DP. Techno-economic assessment of coal-or biomass-fired oxy-combustion power plants with supercritical carbon dioxide cycle. Energy Conversion and Management. 2020;221:113143.